

FULL PAPER

Open Access



Plasma frequency demand for mode conversion processes from slow Z-mode to LO-mode waves in an inhomogeneous plasma

Mohammad Javad Kalaei^{1*}  and Yuto Katoh²

Abstract

The mode conversion process responsible for radio wave generation has been studied for several decades; however, the properties of the condition required for an efficient conversion process are still unknown. The aim of this study is to determine the value of plasma frequency required for an efficient mode conversion process from slow Z-mode to left-hand ordinary (LO)-mode waves in the matching cases, where the two branches of the dispersion relation of the two modes are perfectly connected. We derive the dispersion relations for electromagnetic wave propagation in an inhomogeneous plasma considering Snell's law and investigated them in detail. We quantify the minimum variation of plasma frequency required for the efficient mode conversion process, which we call "the plasma frequency demand." We show that the condition required for the efficient mode conversion can be satisfied by waves propagating first toward the high-density region and then returning toward the low-density region before reaching the region where the wave frequency matches the cutoff frequency; therefore, a large inhomogeneity is not always required. We show that the angle between the background magnetic field and the density gradient has a significant effect on the plasma frequency demand.

Keywords: Inhomogeneity, Mode conversion, Z-mode, LO-mode, Snell's law

Main text

Introduction

The mode conversion responsible for radio wave generation has been studied for several decades (e.g., Oya 1971, 1974; LaBelle 2018) and owing to the importance of this subject, it is still an active topic in a lot of research. It is well known that the refractive index is determined by the characteristics of the wave, such as wave frequency and wave normal angle, and by the parameters of the plasma medium, such as number density of plasma and background magnetic field strength (Stix 1992). The mode conversion of slow Z-mode waves ($\omega_p < \omega < \omega_{\text{UHR}}$,

where ω , ω_p , and ω_{UHR} are the wave frequency, electron plasma frequency, and upper hybrid resonance frequency, respectively) to left-hand ordinary (LO)-mode waves has been investigated for the purpose of understanding the origin of the planetary radio emissions (Jones 1976, 1980, 1987, 1988), Jovian decametric radiation (Oya 1974; Jones 1977), and auroral kilometric radiation (Benson 1975).

Recent simulation studies investigated the mode conversion process in detail and revealed the condition required for the efficient mode conversion quantitatively (Kim et al. 2005; Kalaei et al. 2009, 2010; Kalaei and Katoh 2014, 2016a, 2019; Horký et al. 2018; Horký and Omura 2019). Jones (1980) considered the condition for the mode conversion under the assumption that the magnetic field direction is perpendicular to the density

*Correspondence: mjkalaei@ut.ac.ir

¹ Space Physics Group, Institute of Geophysics, University of Tehran, Tehran, Iran

Full list of author information is available at the end of the article

gradient and derived a formula for the beaming angle of LO-mode waves. Kalaei and Katoh (2014, 2016a) compared the beaming angle proposed by Jones (1980) to the angle obtained by simulation results and proposed an improvement of the beaming angle theory. Kalaei and Katoh (2016b) considered the magnetic field direction arbitrary to the density gradient to generalize the condition for the mode conversion and presented the formula for the beaming angle of LO-mode waves. The sequence of the conversion process from Z-mode to LO-mode waves is illustrated in Fig. 1. First, let us consider a situation where slow Z-mode waves of frequency ω propagate toward a region of higher plasma density. These waves become fast Z-mode waves after passing through the layer with $\omega = \omega_p$. Although fast Z-mode waves of frequency ω can exist in the higher density region as long as the wave frequency is higher than the Z-mode wave cutoff frequency $\omega_{Z\text{-cutoff}}$, the waves change their propagation direction toward the lower density region before reaching the region where $\omega = \omega_{Z\text{-cutoff}}$ and then

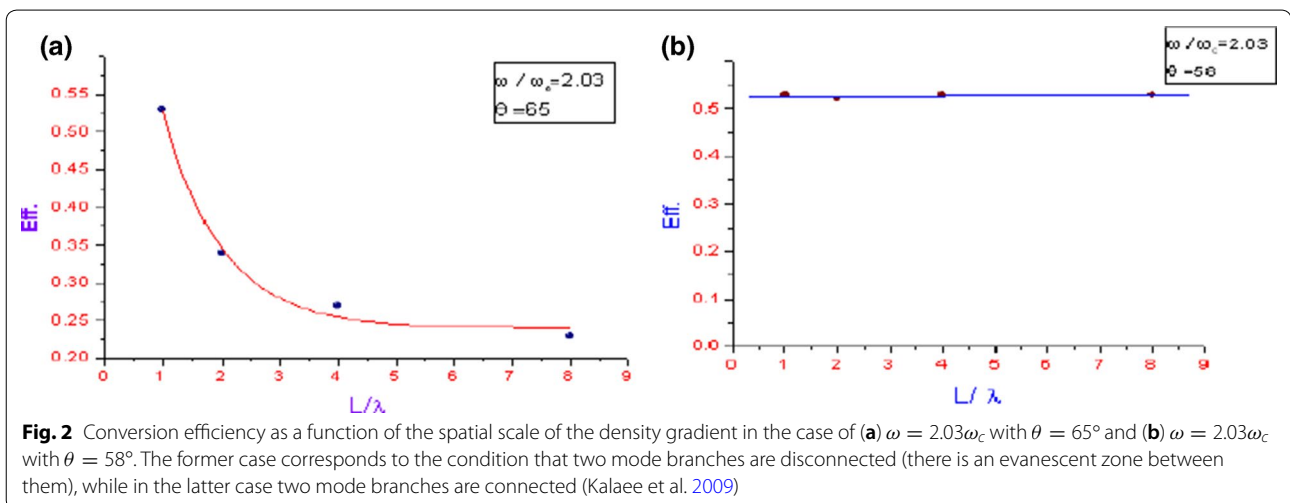
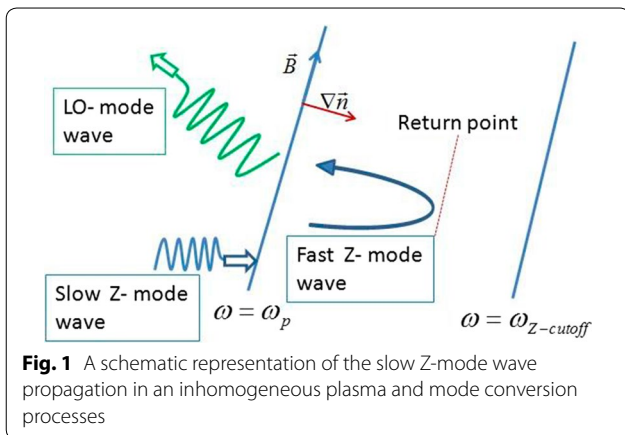
propagate further into the lower density region passing through the layer with $\omega = \omega_p$, where the waves have the possibility to convert into LO-mode waves.

Kalaei et al. (2009) performed several simulations with different steepness and revealed the conversion efficiency as shown in Fig. 2, where L/λ shows the steepness of the inhomogeneity, L is the scale length of the density gradient, and λ is the wavelength of incident waves. For the case in which the two branches of modes are separated, a region of evanescence develops between the two branches, and mode conversion can only take place by the tunneling effect. Therefore, for an efficient mode conversion in this case, the steepness of the inhomogeneity is important (Fig. 2a). However, for the case in which the two mode branches are connected, the steepness is not critical and the conversion efficiency is determined independently of the steepness (Fig. 2b).

In this paper, we focus on the return point of the waves where the plasma density becomes the highest along a ray-path in the mode conversion process. We consider the condition of the mode conversion employing the dispersion relation of cold plasma and Snell's law. By assuming the conditions in which the two mode branches are connected where the mode conversion can occur with the highest efficiency, we formulate the minimum variation of the plasma frequency needed for this efficient conversion process, which we call "the plasma frequency demand," and quantify the range of wave frequency of the incident slow Z-mode waves.

Theory and assumptions

First, we review the coupling properties of the Z-mode and LO-mode waves based on the cold plasma theory, and then we extend our discussion to formulate the plasma frequency for the mode conversion processes.



The dispersion relation of waves in a cold plasma is given by

$$n^2 = n_{\parallel}^2 + n_{\perp}^2 = 1 - \frac{2X(X-1)}{2(X-1) - Y^2 \sin^2 \theta \pm \Gamma}, \quad (1)$$

where n_{\parallel} and n_{\perp} are the parallel and perpendicular components of the refractive index, respectively, $\Gamma = [Y^4 \sin^4 \theta + 4(X-1)^2 Y^2 \cos^2 \theta]^{\frac{1}{2}}$, $X = (\frac{\omega_p}{\omega})^2$, $Y = \frac{\omega_c}{\omega}$, ω_c is the electron gyrofrequency, θ is the wave normal angle, and the +(-) sign indicates the refractive index of the extraordinary (ordinary) mode. The ordinary and extraordinary modes coalesce under the condition where $\Gamma = 0$. This in turn requires that the conditions of $\theta = 0$ and $X = 1$ be simultaneously satisfied:

$$\Gamma = [4(X-1)^2 Y^2]^{\frac{1}{2}} = 2(X-1)Y \quad (2)$$

and

$$n^2 = n_{\parallel}^2 = 1 - \frac{2X(X-1)}{2(X-1) + 2(X-1)Y} = 1 - \frac{X}{1+Y} \quad (3)$$

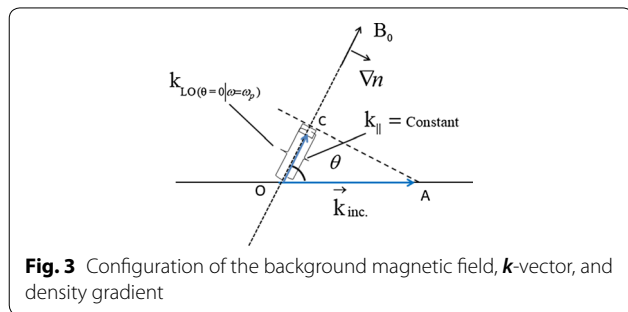
and then for $X \rightarrow 1$, $\Gamma = 0$ and $n^2 = n_{\parallel}^2 = \frac{Y}{1+Y}$.

That is, at this point (mode conversion point), $\omega_p = \omega$ and the wave normal angle should be zero ($n_{\perp} = 0$). Meanwhile, by considering Snell's law and the assumption that the external magnetic field is directed perpendicular to the density gradient, the parallel component of the refractive index should be constant during the wave propagation in an inhomogeneous plasma. Figure 3 shows the configuration of the background magnetic field B_0 , k -vector, and the density gradient ∇N , where B_0 is assumed to be perpendicular to ∇N .

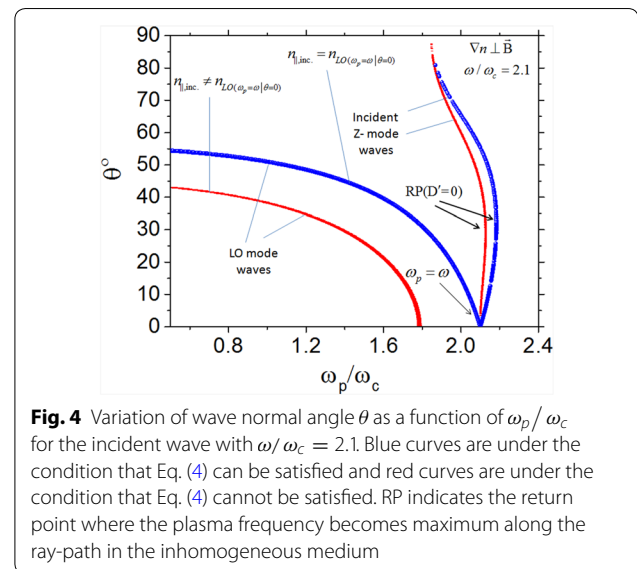
The above discussion results in a condition for effective mode conversion,

$$n_{\parallel,inc} = \text{constant} = n_{LO(\omega_p = \omega | \theta = 0)}, \quad (4)$$

where $n_{\parallel,inc}$ represents the parallel component of the refractive index of the incident wave and $n_{\omega_p = \omega | \theta = 0}$ denotes the LO-mode refractive index at the mode



conversion point, where $\omega_p = \omega$ and $\theta = 0$. It has been suggested that for a certain incident angle of waves, the two wave mode branches (ordinary and extraordinary) are connected and the condition required for the efficient mode conversion is satisfied. Figure 4 shows the wave normal angle θ of the ordinary and extraordinary mode waves of frequency $\omega/\omega_c = 2.1$ as a function of ω_p/ω_c , determined from the dispersion relation of cold plasma considering Snell's law. One case is under the condition that Eq. (4) is satisfied (blue curves) and the other case is under the condition that Eq. (4) is not satisfied (red curves). In the first case, $n_{\parallel,inc} = \text{constant} = n_{LO(\omega_p = \omega | \theta = 0)} = 0.567$, while in the second case, $n_{\parallel,inc} = \text{constant} = 0.714 \neq n_{LO(\omega_p = \omega | \theta = 0)} = 0.567$. It can be observed from Fig. 4 that in the first case, the two wave modes are coupled (which leads to efficient mode conversion) and in the second case, the two wave modes are decoupled (which leads to weak mode conversion). In the second case, the mode conversion can only occur via the tunneling effect, where the steepness of inhomogeneity becomes important (Kalaei and Katoh 2014). In the first case, where the two wave modes are coupled, the efficient mode conversion can be expected regardless of the steepness of the inhomogeneity (Kalaei et al. 2009). However, even in the first case, the plasma frequency required is crucial in the mode conversion process. Here, one fundamental question arises from the discussion above: how large is the inhomogeneity of plasma required for mode conversion under the condition that Eq. (4) is satisfied? In the next section, we extend our discussion to formulate the plasma frequency required for the efficient mode conversion to occur.



Calculation of the plasma frequency demand

We start from the dispersion relation in the cold plasma with Snell's law, and then we consider the return point. The dispersion relation is given by

$$D(n, \omega) = An^4 + Bn^2 + C = 0, \quad (5)$$

where $A, B,$ and C are coefficients including $\omega_p, \omega_c, \omega,$ and θ . The refractive index can be described by the parallel and perpendicular components given by $n^2 = n_{\parallel}^2 + n_{\perp}^2$, where $\sin \theta = \frac{n_{\perp}}{n}$ and $\cos \theta = \frac{n_{\parallel}}{n}$. Thus, we rewrite Eq. (5) as

$$A \left(n_{\parallel}^2 + n_{\perp}^2 \right)^2 - B \left(n_{\parallel}^2 + n_{\perp}^2 \right) + C = 0, \quad (6)$$

$$\begin{aligned} A &= S \sin^2 \theta + P \cos^2 \theta \\ B &= RL \sin^2 \theta + PS(1 + \cos^2 \theta), \\ C &= PRL \end{aligned} \quad (7)$$

where $R = 1 - \tilde{\omega}_p^2 / (1 + \tilde{\omega}_c), L = 1 - \tilde{\omega}_p^2 / (1 - \tilde{\omega}_c), P = 1 - \tilde{\omega}_p^2, S = (R + L) / 2,$ and $\tilde{\omega}_p$ and $\tilde{\omega}_c,$ respectively, describe the plasma frequency and gyrofrequency normalized by the wave frequency ω . By making use of the above equations, Eq. (6) can be rewritten in the form of

$$Sn_{\perp}^4 + [(S+P)n_{\parallel}^2 - RL - PS]n_{\perp}^2 + P(n_{\parallel}^4 - 2Sn_{\parallel}^2 - RL) = 0. \quad (8)$$

By considering n_{\parallel} as a constant (projection on the boundary surface), Eq. (6) is rewritten in the form

$$A'n_{\perp}^4 + B'n_{\perp}^2 + C' = 0, \quad (9)$$

where $A', B',$ and C' are defined by

$$A' = 1 - \tilde{\omega}_p^2 - \tilde{\omega}_c^2 \quad (10)$$

$$B' = \left[(1 - \tilde{\omega}_p^2)(1 - \tilde{\omega}_c^2) + (1 - \tilde{\omega}_p^2 - \tilde{\omega}_c^2) \right] n_{\parallel}^2 - (1 - \tilde{\omega}_p^2)^2 - (1 - \tilde{\omega}_p^2)(1 - \tilde{\omega}_p^2 - \tilde{\omega}_c^2) + \tilde{\omega}_c^2 \quad (11)$$

$$C' = (1 - \tilde{\omega}_p^2) \left[n_{\parallel}^4 (1 - \tilde{\omega}_c^2) - 2n_{\parallel}^2 (1 - \tilde{\omega}_p^2 - \tilde{\omega}_c^2) + (1 - \tilde{\omega}_p^2)^2 - \tilde{\omega}_c^2 \right]. \quad (12)$$

As we are interested in the plasma frequency at the return point (indicated by RP in Figs. 4, 5), we consider the situation in Eq. (9) to find the return point. At the return point, Eq. (9) has two equal, non-zero solutions. The solutions do not correspond to the mode conversion between the ordinary and extraordinary modes, but merely correspond to the return of the extraordinary mode. Thus, for this case, the condition is given

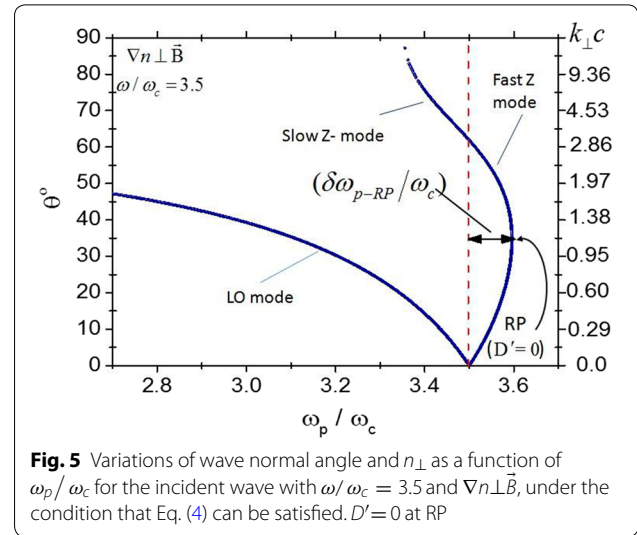


Fig. 5 Variations of wave normal angle and n_{\perp} as a function of ω_p / ω_c for the incident wave with $\omega / \omega_c = 3.5$ and $\nabla n_{\perp} \perp \vec{B}$, under the condition that Eq. (4) can be satisfied. $D' = 0$ at RP

by $D' = B'^2 - 4A'C' = 0$. By substituting Eqs. (10), (11), and (12) in Eq. (9) and after simplifications, we obtain

$$D' = \tilde{\omega}_p^4 \tilde{\omega}_c^2 \left[\tilde{\omega}_c^2 (1 - n_{\parallel}^2)^2 + 4(1 - \tilde{\omega}_p^2) n_{\parallel}^2 \right] = 0 \quad (13)$$

and then

$$\tilde{\omega}_c^2 (1 - n_{\parallel}^2)^2 + 4(1 - \tilde{\omega}_p^2) n_{\parallel}^2 = 0 \quad (14)$$

$$\tilde{\omega}_c^2 (1 - n_{\parallel}^2)^2 = -4(1 - \tilde{\omega}_p^2) n_{\parallel}^2. \quad (15)$$

By solving Eq. (15) for $\tilde{\omega}_p$, we obtain

$$\tilde{\omega}_p^2 = 1 + \frac{\tilde{\omega}_c^2 (1 - n_{\parallel}^2)^2}{4n_{\parallel}^2} \quad (16)$$

or

$$\left(\frac{\omega_{p-RP}}{\omega_c} \right)^2 = \left(\frac{\omega}{\omega_c} \right)^2 + \frac{(1 - n_{\parallel}^2)^2}{4n_{\parallel}^2}. \quad (17)$$

Equations (16, 17) indicate the value of ω_p at the return point. The initial condition for the occurrence of efficient mode conversion (that the ordinary and extraordinary modes are connected) is

$$n_{\parallel}^2 = n_{LO(\omega_p = \omega | \theta=0)}^2 = \frac{1}{1 + \frac{\omega}{\omega_c}}. \quad (18)$$

Finally, by substituting Eq. (18) in Eq. (17), we obtain

$$\left(\frac{\omega_{p-RP}}{\omega_c}\right)^2 = \left(\frac{\omega}{\omega_c}\right)^2 + \frac{\left(\frac{\omega}{\omega_c}\right)^2}{4\left(\frac{\omega}{\omega_c} + 1\right)} \quad (19)$$

or

$$\frac{\omega_{p-RP}}{\omega_c} = \left[\left(\frac{\omega}{\omega_c}\right)^2 + \frac{\left(\frac{\omega}{\omega_c}\right)^2}{4\left(\frac{\omega}{\omega_c} + 1\right)} \right]^{1/2}. \quad (20)$$

The above equation shows the value of the plasma frequency at the return point in an efficient mode conversion event (the condition Eq. (18) is satisfied). Figure 5 shows another example of efficient mode conversion. The initial angular frequency of the slow Z-mode wave is $3.5\omega_c$ with the wave normal angle $\theta \leq 61.8^\circ$ in the region where $\omega_p < 3.5\omega_c$ ($3.35\omega_c < \omega_p < 3.5\omega_c$). The plasma frequency at the return point indicated by RP can be obtained from Eq. (20). Here, we define another parameter $\delta\omega_{p-RP}$, which we call “the plasma frequency demand,” corresponding to the difference between the plasma frequency at the return point and the plasma frequency at the point where $\omega_p = \omega$, which is given by

$$\frac{\delta\omega_{p-RP}}{\omega_c} = \frac{\omega_{p-RP}}{\omega_c} - \frac{\omega_p}{\omega_c} \Big|_{\omega_p=\omega}. \quad (21)$$

Using Eqs. (20) and (21), we obtain $\omega_{p-RP} \approx 3.56\omega_c$ and $\delta\omega_{p-RP} \approx 0.1\omega_c$ for the above case, as shown in Fig. 5.

Using Eq. (21), we obtain the values of $\frac{\delta\omega_{p-RP}}{\omega_c}$ for a wide range of angular frequency of the incident slow Z-mode waves, $0.1\omega_c \leq \omega \leq 100\omega_c$, for the occurrence of efficient mode conversion. The results are shown in Fig. 6 as the blue solid line. The red solid line in Fig. 6 indicates the difference between the plasma frequency at the cutoff of Z-mode waves ($\omega_{p-Z-cutoff}$) and the frequency of the incident wave, ($\delta\omega_{p-Z-cutoff}/\omega_c = \frac{\omega_{p-Z-cutoff}-\omega}{\omega_c}$), where the Z-mode cutoff frequency is given by $\omega_{Z-cutoff} = -\frac{\omega_c}{2} + \left[\frac{\omega_c^2}{4} + \omega_{p-Z-cutoff}^2\right]^{1/2}$. Under the condition that the efficient mode conversion can occur, the $\delta\omega_{p-RP}$ required for the mode conversion is not necessarily large compared to the $\delta\omega_{p-Z-cutoff}$ required to reach the Z-mode cutoff frequency. $\delta\omega_{p-RP}$ is estimated to

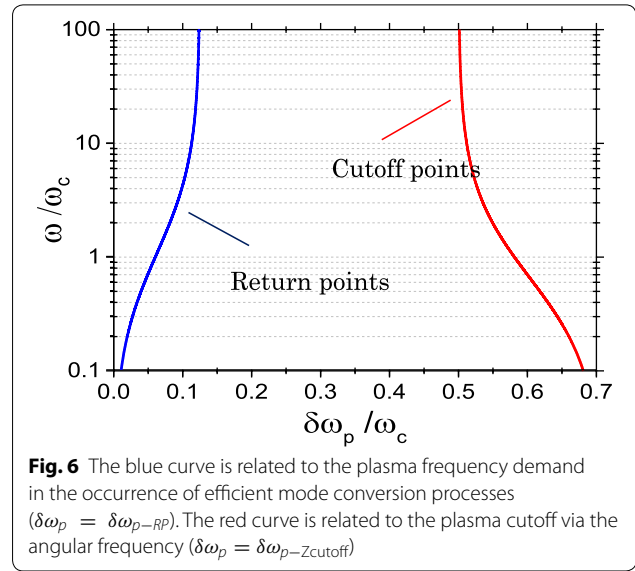


Fig. 6 The blue curve is related to the plasma frequency demand in the occurrence of efficient mode conversion processes ($\delta\omega_p = \delta\omega_{p-RP}$). The red curve is related to the plasma cutoff via the angular frequency ($\delta\omega_p = \delta\omega_{p-Zcutoff}$)

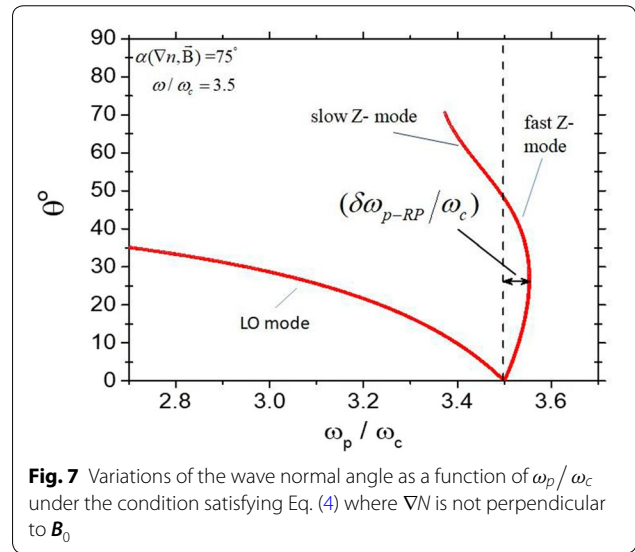


Fig. 7 Variations of the wave normal angle as a function of ω_p/ω_c under the condition satisfying Eq. (4) where ∇N is not perpendicular to B_0

range from $0.01\omega_c$ to $0.12\omega_c$ for ω ranging from $0.1\omega_c$ to $100\omega_c$.

Finally, we consider the case where the magnetic field direction is not purely perpendicular to the density gradient and obtain the plasma frequency at the return point numerically. Figure 7 shows variations of the wave normal angle as a function of ω_p/ω_c for the incident wave with $\omega/\omega_c = 3.5$, where the angle α between ∇N and B_0 is 75° , under the condition that Eq. (4) is satisfied (the two mode branches are connected). In this example, $\delta\omega_{p-RP}$ is estimated to be $0.053\omega_c$, which is less than in the case of the previous example ($\alpha = 90^\circ$).

Summary

The inhomogeneity plays an important role in the mode conversion process. We aim to quantify the least frequency of plasma under the condition satisfying the efficient mode conversion, which we call “the plasma frequency demand.” We described how the wave that leads to efficient mode conversion propagates in the inhomogeneous plasma. We studied how the ray-path of the Z-mode waves changes before reaching the cutoff frequency and then reflects into the plasma frequency layer with $\omega_p = \omega$. Using the dispersion relation for waves in cold plasma according to Snell’s law, we considered the return point of waves under the assumption that the external magnetic field is directed perpendicular to the density gradient. We obtained the formula to quantify the least plasma frequency required for efficient mode conversion. The results which we obtained are summarized as follows:

1. We formulated the plasma frequency at the reflected point (Eq. 20) and “the plasma frequency demand” for the efficient mode conversion (Eq. 21).
2. The range of $\delta\omega_{p-RP}$ is between $0.01\omega_c$ and $0.12\omega_c$ for the slow Z-mode of incident waves ranging from $0.1\omega_c$ to $100\omega_c$, under the assumption that the magnetic field direction is purely perpendicular to the density gradient.
3. $\delta\omega_{p-RP}$ becomes small for the case in which the angle between the magnetic field direction and the density gradient is not purely perpendicular. We obtained $\delta\omega_{p-RP} \approx 0.053$ with $\alpha = 75^\circ$ and $\omega_p > \omega_c$, which is less than the $\delta\omega_{p-RP} \approx 0.1$ that we obtained in the case with $\alpha = 90^\circ$.

Finally, for the case where Eq. (4) is not satisfied, corresponding to the condition in which the two mode branches are separated and an evanescent layer develops between the two wave modes, the mode conversion can occur by the tunneling effect (Kalaei and Katoh 2014). In this case, the steepness of the inhomogeneity plays an important role in controlling the efficiency of the mode conversion.

The relationship between the density gradient and the conversion efficiency suggested by the present study should be examined by comparison with in situ observations. The evaluation of the properties of the observed Z-mode and LO-mode waves and the condition of the ambient plasma, comparing them with those expected from the theoretical consideration, are also important (e.g., Kalaei et al. 2010) to discuss the dominance of the connected/disconnected cases, the assumption of the spatial distributions of plasma density and background magnetic field, and the frequency/wavenumber spectra

of the incident upper hybrid mode waves considering the amplitude ratio between the incident waves and converted radio waves. We need to know the variation of the wave normal angle as a function of ω_p/ω_c , as indicated in Fig. 5. For the case of the mode conversion satisfying the matching condition, we expect the variation of the wave normal angle of Z-mode waves in the observation results. The wavenumber spectra can be estimated by the ratio of the wave electric field components to the wave magnetic field components with reference to the dispersion relation. For the intensities of both the incident waves and converted radio waves, we need to carefully select events where we can assume that both the observed radio waves and Z-mode waves in the vicinity of the plasmopause are closely related to each other. Regarding the angle between the direction of the density gradient and the wave normal angle, in a first step, we will assume that the density gradient is perpendicular to the background magnetic field. This assumption is basically acceptable in the equatorial region of the plasmopause. A close comparison between theoretical/simulation studies and observation results is crucial. Arase, the exploration of energization and radiation in geospace (ERG) satellite (Miyoshi et al. 2018) orbits the inner magnetosphere and crosses the plasmopause, where efficient mode conversion can occur. The Arase satellite is capable of observing radio emissions of LO- and Z-mode waves (Kasaba et al. 2017; Kasahara et al. 2018a; Kumamoto et al. 2018; Matsuda et al. 2018), energetic electrons (Kazama et al. 2017; Kasahara et al. 2018b) serving free energy to excite slow Z-mode waves, and the energy exchange between waves and particles (Katoh et al. 2018; Hikishima et al. 2018). We expect that the comparison between the theory and the Arase satellite observations will enable us to investigate a comprehensive scenario of the mode conversion process. The discussion on the percentage of radio waves satisfying the matching condition is highly important. It is beyond the scope of this study, but it is a very important aspect to be addressed in our future work.

Abbreviations

LO: Left-hand ordinary; ERG: Exploration of energization and radiation in geospace.

Acknowledgements

This work was carried out by the “Computational Joint Research Program (Collaborative Research Project on Computer Science with High-Performance Computing)” at the Institute for Space-Earth Environmental Research, Nagoya University. The computer simulation was performed on the KDK computer system at the Research Institute for Sustainable Humanosphere, Kyoto University and the computational resources of the HPCI system provided by the Research Institute for Information Technology, Kyushu University; the Information Technology Center, Nagoya University; and the Cyberscience Center, Tohoku University, through the HPCI System Research Project (Project ID: hp160131, hp170064, hp180035, and hp190074). YK is supported by

Grants-in-Aid for Scientific Research (15H05815, 15H05747, 17K18798, and 18H03727) of the Japan Society for the Promotion of Science.

Authors' contributions

MJK contributed with the theoretical consideration and data analysis. YK contributed with the discussion of the theoretical consideration. Both authors read and approved the final manuscript.

Funding

This study is supported by Grants-in-Aid for Scientific Research (15H05747, 15H05815, 17K18798 and 18H03727) of the Japan Society for the Promotion of Science.

Availability of data and materials

The data used in this paper can be obtained upon request to the corresponding author.

Competing interests

The authors declare that they have no competing interests.

Author details

¹ Space Physics Group, Institute of Geophysics, University of Tehran, Tehran, Iran. ² Department of Geophysics, Graduate School of Science Tohoku University, Sendai, Japan.

Received: 28 December 2019 Accepted: 30 June 2020

Published online: 10 July 2020

References

- Benson RF (1975) Source mechanism for terrestrial kilometric radiation. *Geophys Res Lett* 2:52–55
- Hikishima M, Kojima H, Katoh Y, Kasahara Y, Kasahara S, Mitani T, Higashio N, Matsuoka A, Miyoshi Y, Asamura K, Takashima T, Yokota S, Kitahara M, Matsuda S (2018) Data processing in software-type wave-particle interaction analyzer onboard the arase satellite. *Earth Planets Space* 70(80):1–12. <https://doi.org/10.1186/s40623-018-0856-y>
- Horký M, Omura Y (2019) Novel nonlinear mechanism of the generation of non-thermal continuum radiation. *Phys Plasmas* 26:022904
- Horký M, Omura Y, Santolík O (2018) Particle simulation of electromagnetic emissions from electrostatic instability driven by an electron ring beam on the density gradient. *Phys Plasmas* 25:042905
- Jones D (1976) Source of terrestrial non-thermal radiation. *Nature* 260:686–689
- Jones D (1977) Mode-coupling of Z-mode waves as a source of terrestrial kilometric and Jovian decametric radiations. *Astron Astrophys* 55:245–252
- Jones D (1980) Latitudinal beaming of planetary radio emissions. *Nature* 288:225–229
- Jones D (1988) Planetary radio emissions from low magnetic latitudes observations and theories, in *Planetary Radio Emissions II*, edited by Rucker HO, Bauer SJ, and Pedersen BM, 255–293, Austrian Acad. Sci., Vienna, Austria
- Jones D, Calvert W, Gurnett DA, Huff RL (1987) Observed, beaming of terrestrial myriametric radiation. *Nature* 328:391–395
- Kalaei MJ, Katoh Y (2014) A simulation study on the mode conversion process from slow Z-mode to LO mode by the tunneling effect and variations of beaming angle. *Adv Space Res* 54:2218–2223
- Kalaei MJ, Katoh Y (2016a) The role of deviation of magnetic field direction on the beaming angle: extending of beaming angle theory. *J Atmos Sol Terr Phys*. 142:35–42
- Kalaei MJ, Katoh Y (2016b) Study of a condition for the mode conversion from purely perpendicular electrostatic waves to electromagnetic waves. *Phys Plasmas* 23:072119
- Kalaei MJ, Katoh Y (2019) A discussion on the mode conversion from purely perpendicular upper-hybrid mode waves to LO mode waves in an inhomogeneous plasma. *Adv Space Res* 64:1732–1739
- Kalaei MJ, Ono T, Katoh Y, Iizima M, Nishimura Y (2009) Simulation of mode conversion from UHR-mode wave to LO-mode wave in an inhomogeneous plasma with different wave normal angles. *Earth Planets Space* 61:1243–1254
- Kalaei MJ, Katoh Y, Kumamoto A, Ono T (2010) Simulation of mode conversion from upper-hybrid waves to LO-mode waves in the vicinity of the Plasmopause. *Ann Geophys* 28:1289–1297
- Kasaba Y, Ishisaka K, Kasahara Y, Imachi T, Yagitani S, Kojima H, Matsuda S, Shoji M, Kurita S, Hori T, Shinbori A, Teramoto M, Miyoshi Y, Nakagawa T, Takahashi N, Nishimura Y, Matsuoka A, Kumamoto A, Tsuchiya F, Nomura R (2017) Wire Probe Antenna (WPT) and Electric Field Detector (EFD) of Plasma Wave Experiment (PWE) aboard ARASE: specifications and Initial Evaluation results. *Earth Planets Space*. <https://doi.org/10.1186/s40623-017-0760-x>
- Kasahara S, Yokota S, Mitani T, Asamura K, Hirahara M, Shibano Y, Takashima T (2018a) Medium-energy particle experiments—electron analyzer (MEPE) for the exploration of energization and radiation in geospace (ERG) mission. *Earth Planets Space* 70(69):1–16. <https://doi.org/10.1186/s40623-018-0847-z>
- Kasahara Y, Kasaba Y, Kojima H, Yagitani S, Ishisaka K, Kumamoto A, Tsuchiya F, Ozaki M, Matsuda S, Imachi T, Miyoshi Y, Hikishima M, Katoh Y, Ota M, Shoji M, Matsuoka A, Shinohara I (2018b) The plasma wave experiment (PWE) on board the arase (ERG) satellite. *Earth Planets Space* 70(86):1–28. <https://doi.org/10.1186/s40623-018-0842-4>
- Katoh Y, Kojima H, Hikishima M, Takashima T, Asamura K, Miyoshi Y, Kasahara Y, Kasahara S, Mitani T, Higashio N, Matsuoka A, Ozaki M, Yagitani S, Yokota S, Matsuda S, Kitahara M, Shinohara I (2018) Software-type wave-particle interaction analyzer on board the arase satellite. *Earth Planets Space*. <https://doi.org/10.1186/s40623-017-0771-7>
- Kazama Y, Wang B-J, Wang S-Y, Ho PTP, Tam SWY, Chang T-F, Chiang C-Y, Asamura K (2017) Low-energy particle experiments—electron analyzer (LEPE) onboard the Arase spacecraft. *Earth Planets Space* 69(165):1–13. <https://doi.org/10.1186/s40623-017-0748-6>
- Kim KS, Kim EH, Lee DH, Kim K (2005) Conversion of ordinary and extraordinary waves into upper hybrid waves in inhomogeneous plasma. *Phys Plasmas* 12:052903
- Kumamoto A, Tsuchiya F, Kasahara Y, Kasaba Y, Kojima H, Yagitani S, Ishisaka K, Imachi T, Ozaki M, Matsuda S, Shoji M, Matsuoka A, Katoh Y, Miyoshi Y, Obara T (2018) High frequency analyzer (HFA) of plasma wave experiment (PWE) onboard the arase spacecraft. *Earth Planets Space* 70(82):1–14. <https://doi.org/10.1186/s40623-018-0854-0>
- LaBelle J (2018) Polarization measurements of unusual cases of medium frequency burst emissions extending below 1.5 MHz. *Earth Planets Space*. 70(143):1–8. <https://doi.org/10.1186/s40623-018-0912-7>
- Matsuda S, Kasahara Y, Kojima H, Kasaba Y, Yagitani S, Ozaki M, Imachi T, Ishisaka K, Kumamoto A, Tsuchiya F, Ota M, Kurita S, Miyoshi Y, Hikishima M, Matsuoka A, Shinohara I (2018) Onboard software of plasma wave experiment aboard arase: instrument management and signal processing of waveform capture/onboard frequency analyzer. *Earth Planets Space* 70(75):1–22. <https://doi.org/10.1186/s40623-018-0838-0>
- Miyoshi Y, Shinohara I, Takashima T, Asamura K, Higashio N, Mitani T, Kasahara S, Yokota S, Kazama Y, Wang S-Y, Tam SWY, Ho PTP, Kasahara Y, Kasaba Y, Yagitani S, Matsuoka A, Kojima H, Katoh Y, Shiokawa K, Seki K (2018) Geospace exploration project ERG. *Earth Planets Space* 70(101):1–13. <https://doi.org/10.1186/s40623-018-0862-0>
- Oya H (1971) Conversion of electrostatic plasma waves into electromagnetic waves: numerical calculation of the dispersion relation for all wavelengths. *Radio Sci*. 12:1131–1141
- Oya H (1974) Origin of Jovian decametric wave emissions—conversion from the electron cyclotron plasma wave to the O-mode electromagnetic wave. *Planet Space Sci* 22:687–708
- Stix TH (1992) *Waves in Plasmas*. American Institute of Physics, New York

Publisher's Note

Springer Nature remains neutral with regard to jurisdictional claims in published maps and institutional affiliations.